Chiang Mai J. Sci. 2014; 41(5.2) : 1274-1286
http://epg.science.cmu.ac.th/ejournal/
Contributed Paper

Graphene Nanoplatelet/Multi-Walled Carbon Nanotube/Polycarbonate Hybrid Nanocomposites for Electrostatic Dissipative Applications: Preparation and Properties

Akkachai Poosala [a], Worrawit Kurdsuk [b], Darunee Aussawasathien*[b] and Duanghathai Pentrakoon*[c]

[a] Technopreneurship and Innovation Management, Graduate School, Chulalongkorn University, Bangkok 10330 Thailand.

[b] Plastics Technology Lab, Polymer Research Unit, National Metal and Materials Technology Center, Pathumthani 12120, Thailand.

[c] Department of Materials Science, Faculty of Science, Chulalongkorn University, Bangkok 10330, Thailand.

*Authors for correspondence; e-mail addresses: (D. Aussawasathien) daruneea@mtec.or.th and (D. Pentrakoon) Duanghat@yahoo.com

Received: 4 July 2013
Accepted: 11 November 2013

Abstract

Graphene nanoplatelet (GNP)/multi-walled carbon nanotube (MWCNT)/polycarbonate (PC) hybrid nanocomposites were prepared via a melt mixing process using a twin screw extruder. The content of GNPs was in the range of 0-2.0 pph of resin (part per hundred resin) whereas the dosage of MWCNTs was kept constant at 0.5 wt%. X-ray diffraction (XRD) showed that GNPs slightly intercalated in the PC matrix since the peak of GNPs at $2\theta = 26.4°$ clearly remained and its intensity increased as the amount of GNPs increased. Transmission electron microscopy (TEM) revealed poor dispersion and intercalation of GNPs in the PC matrix. The nanocomposite containing 0.5 wt% MWCNTs had a measured tribo-charge voltage outside the electrostatic dissipative (ESD) specification. When 0.2-2.0 pph of resin of GNPs were added in MWCNT/PC nanocomposites, the ESD properties were improved and mostly within the specification range. However, the tribo-charge voltage did not show any trend with increased GNP content. The glass transition temperature (T_g) and heat capacity jump at the glass transition stages of the nanocomposites insignificantly changed as the content of GNPs increased. The decomposition temperature (T_d) slightly increased at low GNP loadings and then began to decrease with increasing GNP contents from 0.6-2.0 pph of resin. The decrease of T_d at high GNP content might result from poor dispersion of GNPs in the PC matrix causing hot spot defects. The melt flow index (MFI) of GNP/MWCNT/PC nanocomposites tended to decrease as the content of GNPs increased due to the formation of a nanoplatelet network which obstructed the motion of polymer chains. This work opens up the possibility of using GNP/

MWCNT/PC nanocomposites in ESD applications. However, suitable surface modification of GNPs is required to improve the dispersion and intercalation of GNPs in the PC matrix.

Keywords: Graphene; Muti-wall carbon nanotube; Polycarbonate; Nanocomposite

1. INTRODUCTION

Electronic components are liable to damage from electrostatic discharge (ESD). A variety of materials has been developed to package sensitive electronic devices and prevent damage during storage and shipping. Electrostatic dissipating thermoplastic composites have successfully eliminated ESD failures in many applications in the electronics industry. Various conductive fillers are currently available to material engineers, including carbon black (CB), carbon fibers (CF), carbon nanotubes (CNT), metallic powders, flakes or fibers, and glass spheres or glass fibers coated with metals [1]. The conductivity of ESD composites depends not only on the filler type and concentration, but also on the specific polymer matrix used and on the generated morphology [2]. High amount of carbon fillers can cause local variation of the filler concentration, resulting in variation of the conductivity with location in the same product. Moreover, high carbon filler content has a negative effect on the processability and mechanical properties of a composite: the melt viscosity increases and the impact resistance decreases. Contamination is also an important issue since the carbon powder tends to slough and thus contaminate the environment in high filled composites. Therefore, it is a challenge to develop cleaner ESD composites with consistent and uniform surface resistivity in the ESD range.

Carbon nanotube (CNT) with a cylindrical nanostructure and graphene with a two-dimensional sheet of sp^2-hybridized carbon atoms densely packed in a honeycomb network have distinctly different geometry; but they have remarkable properties, such as superior thermal and mechanical properties and exceptional electronic transport [3-8], which make them excellent candidates as reinforcing and conducting fillers in composite materials. Recently, theoretical and experimental studies on polymer composites containing CNTs have been carried out [9-15]. However, investigation on GNP-filled polymer composites is limited [15-17].

Even though CNT has comparable mechanical properties compared to graphene, graphene remains a better nanofiller than CNT in certain aspects, such as thermal and electrical conductivity [18-21]. It is well known that the morphology of fillers has significant effects on the composite properties [22-24]. For example, Xie et al. [15] revealed that GNP-filled composites exhibited slightly lower percolation threshold and higher electrical conductivity, and could form conductive networks more easily than CNT-filled composites at the same volume fraction of fillers. Furthermore, the properties improvements of polymer/graphene nanocomposites are also obtained at a very low filler loading in the polymer matrix [17, 25-28]. To date, the cost of GNP is relatively more expensive than CNT. Therefore, the GNP/CNT/polymer hybrid system is an alternative means to obtain nanocomposites with balanced properties at economically effective cost.

PC is one of the most important commodity polymers used to make injection moldable composites for ESD applications owing to its good mechanical and thermal properties, and high impact resistance. Moreover, its amorphous characteristic will avoid complexities of interpreting property changes related to crystallization at various nanofiller contents.

Due to the large surface energy and strong interaction, both CNTs and GNPs are difficult

to be uniformly dispersed in a polymer matrix by simply mechanical mixing [29, 30]. Different polymers have been used to produce GNP or CNT filled polymer nanocomposites by a variety of methods such as *in situ* polymerization, solution mixing, and melt processing [24, 27, 28, 31-33]. Among these approaches, the melt mixing technique is a popular method for preparing thermoplastic nanocomposites since no solvent is required and the filler is mixed with the polymer matrix in the molten state.

In the present study, polymer nanocomposites with combinations of GNP/MWCNT/PC were prepared for ESD applications. In our preliminary studies, it was found that PC nanocomposites containing MWCNTs ⩾ 1 wt% had ESD properties such as surface resistivity, tribo-charge voltage, and decay time in the specification ranges. Therefore, GNP was utilized as a co-filler with low contents as possible in the hybrid filler system containing MWCNT less than 1 wt%, e.g. 0.5 wt% to improve ESD properties of PC nanocomposites. The effects of GNP content, distribution, and intercalation on thermal properties, MFI, and ESD properties such as surface resistivity, tribo-charge voltage, and decay time were investigated.

2. MATERIALS AND METHODS

2.1 Materials and Sample Preparation

The injection molding grade of PC resin (Makrolon 2456) was supplied from Bayer MaterialScience, Thailand. PC/MWCNT masterbatch (Plasticyl PC 1501) and GNPs (TNGNP) supplied from Nanocyl, Belgium and Timenano, Republic of China, respectively, were used as nanofillers. All materials were dried in a vacuum oven at 120°C for 2 h under a pressure of 50 mbar and then manually blended in plastic containers before melt processing using a twin screw extruder (Lab-Tech). The contents of GNPs incorporated into PC resin were 0.2, 0.4, 0.6, 0.8, 1.0, 1.5, and 2.0 pph of resin, whereas the dosage of MWCNT was kept constant at 0.5 wt%. The screw diameter, screw length, and screw L/D ratio were 20 mm, 64 cm, and 32, respectively. The set-up temperature of mixing screws was in the range of 240-290°C. The rotation speeds of feeding screws and mixing screws were 12 and 120 rpm, respectively.

All composites were dried in a vacuum oven at 120°C for 2 h under a pressure of 50 mbar before compression molding process. Sheet with a thickness of 1.5 mm was prepared using a hot press (Lab-Tech). The compression temperature was in the range of 290-300°C. Each sample was compressed under pressure of 15 Tonf. The pre-heat and full press times were 15 and 10 min, respectively. Venting was performed 3 times and 1 sec per time. The sample was cooled for 5 min.

2.2 Characterization

The electrical resistivity of injection-molded samples was measured according to ANSI/ESD STM11.13-2004 using a resistance meter (3M-701). The tribo-charge voltage and decay time were determined based on ESD ADV11.2-1995 using an electrostatic voltage meter (Trek-520), and a charged plate monitor system (Trek Model 150A), respectively. All experiments were performed at ambient temperature, 25 ± 2°C. Five specimens were tested for each set of measurements. TGA measurements were carried out using a TA Instruments thermobalance (TGA Q500) under nitrogen atmosphere and at a heating rate of 20°C/min. A differential scanning calorimeter (DSC) (Mettler Toledo, Model-DSC 822^e) was used for the dynamic measurement and data analysis under N_2 flow. A heating rate of 20°C/min was applied to the sample during measurement and the sample was scanned over the temperature range of 25-300°C. The MFI was measured with an extrusion plastometer (Davenport model 10, Lloyd Instruments),

according to ASTM D1238 at 260°C, with a 2.16 kgf weight. The MFI values reported were the average of ten measurements. TEM samples were ultra-thin-sectioned using an ultramicrotome. The morphology of the nanocomposites was obtained using a JEOL JEM-2010, LaB6 filament at an accelerating voltage of 200 kV. Wide-angle X-ray diffraction (WAXD) characterization was carried out via a Rigaku, Model-TTRAX III X-ray diffractometer. The incident X-ray wavelength is 1.54 Å (Cu Kα line) at 50 kV and 300 mA. Samples were scanned over the range of diffraction angles 2θ = 1-45°, with a scan speed of 0.5°/min at room temperature. Raman spectra were recorded using a Senterra Dispersive Raman Microscope (Bruker Optics). The He-Ne laser excitation wavelength was 532 nm with a laser power of ca. 20 mW. The spectral range between 4500-70 cm^{-1} was recorded using TE-Cooled CCD detector.

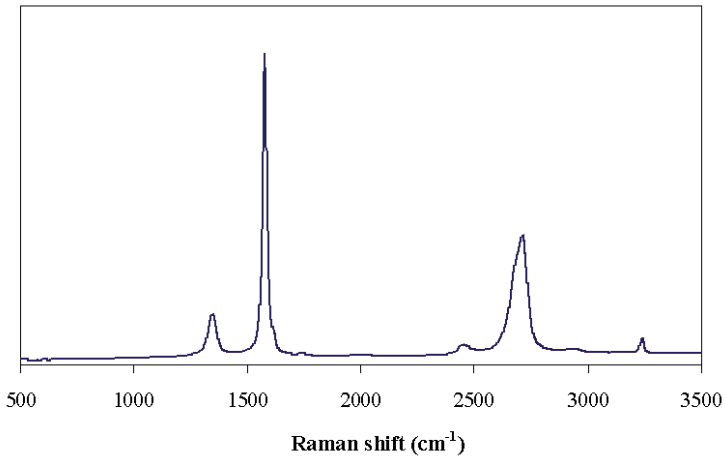

Figure 1. Raman spectra of GNP.

3. RESULTS AND DISCUSSION

3.1 Raman Spectra

Raman spectroscopy was employed to show the graphite structure of GNP. As shown in Figure 1, the first-order Raman spectra of G band had a strong peak at ~ 1578 cm^{-1} and a weak peak of D band at ~ 1346 cm^{-1}. The G band and D band are attributed to the first-order scattering of the E_{2g} vibrational mode in graphite sheets [34] and structural defects (disorder-induced modes), respectively. The second-order spectrum is indicated as 2D band at ~ 2714 cm^{-1} which is the overtone (second harmonic) of the D band [35]. The ratio of D- to G- band intensity (I_D/I_G) of GNP was approximately 0.21. It was reported that the I_D/I_G ratio could be used to qualitatively characterize the change of defects in the carbon nanotubes [13, 36].

3.2 X-Ray Diffraction

Figure 2 illustrates the WAXD patterns of GNP/MWCNT/PC nanocomposites at different GNP loadings. The peak at 2θ = 17° indicated the presence of PC resin in polymer nanocomposites [28]. Dispersion and orientation of GNPs in PC nanocomposites were analyzed from 2-dimensional X-ray scattering. When the intensity was integrated as a function of scattering angle 2θ, a sharp reflection was present at 2θ = 26.4° for GNPs, which corresponds to the interlayer spacing of un-intercalated graphite (d = 0.34 nm) [28].

It is clear that GNPs very slightly inter-

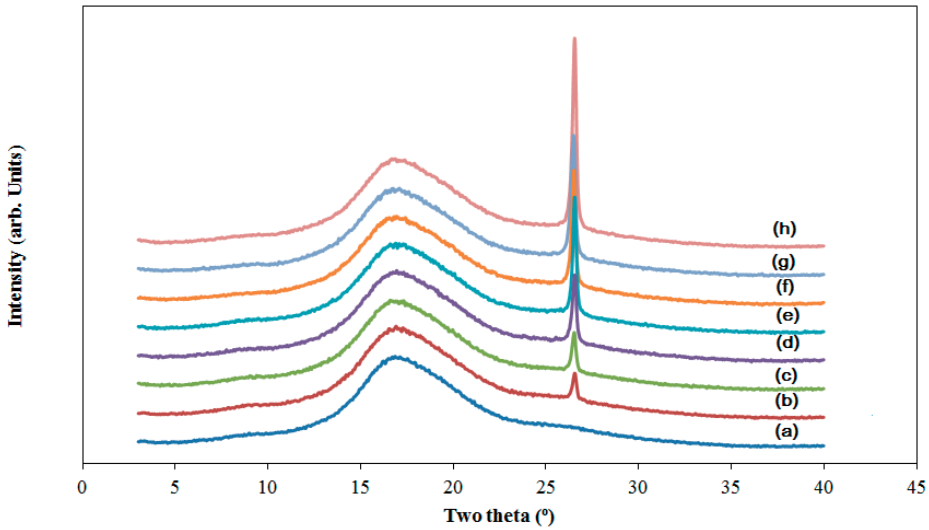

Figure 2. XRD patterns of the GNP/MWCNT/PC nanocomposites with the different GNP contents (pph of resin): (a) 0, (b) 0.2, (c) 0.4, (d) 0.6, (e) 0.8, (f) 1.0, (g) 1.5, and (h) 2.0.

calated in the PC matrix due to van der Waals interactions between graphite planes since the peak of the graphite structure at $2\theta = 26.4°$ was remained and its intensity increased as the amount of GNPs increased. These findings are in good agreement with the results of the literatures, confirming the existence of graphite layers of GNPs in polymer nanocomposites [28, 37].

3.3 TEM Analysis

It is well-known that the homogeneous dispersion of graphene in the polymer matrix plays an important role in influencing the properties of PC. The morphology at high magnification of GNP/MWCNT/PC nanocomposites at different GNP loadings using TEM was observed as shown in Figure 3. The TEM images supported the XRD results indicating

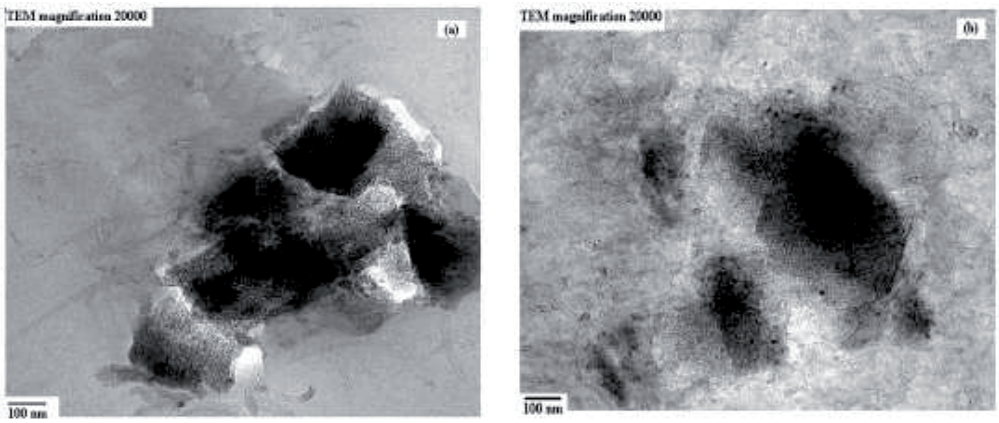

Figure 3. TEM photographs of the GNP/MWCNT/PC nanocomposites with the different GNP contents (pph of resin): (a) 0.2, (b) 0.6, (c) 1.0, and (d) 2.0.

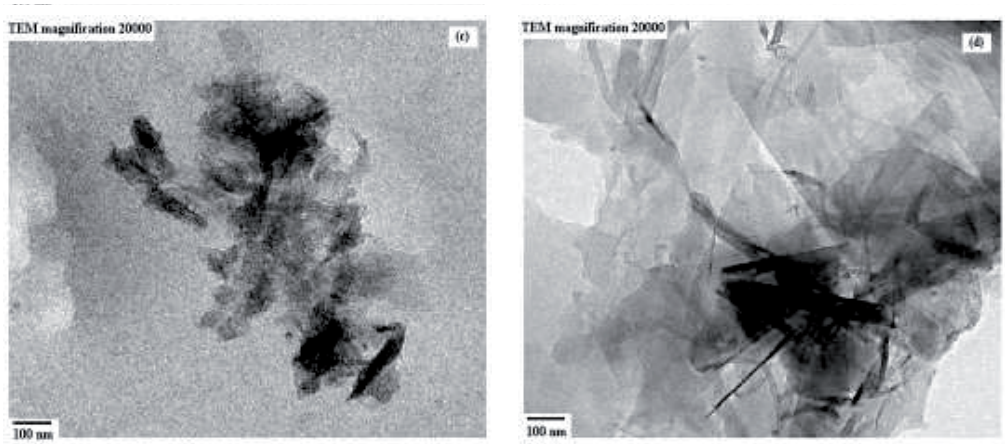

Figure 3. TEM photographs of the GNP/MWCNT/PC nanocomposites with the different GNP contents (pph of resin): (a) 0.2, (b) 0.6, (c) 1.0, and (d) 2.0.

some apparent aggregations and poor intercalation of GNPs in the PC matrix. This might result from no interaction between GNPs and the polar groups of PC since GNPs did not have any functional groups on the surface such as oxygen and hydroxyl groups [37]. The gap between graphene sheets was still narrow. Variation in the level of GNP intercalation in the nanocomposite might cause inconsistent properties of PC nanocomposites.

3.4 ESD Measurement

An ESD control system should be introduced in the production and handling of electronic parts and devices. Static dissipative materials are often used to slow down the charge removal process and prevent a damaging ESD event. The Electronic Industry Association (EIA) specifies that the typical requirements for surface resistivity, tribo-charge voltage, and decay time are 10^6-10^9 Ω/sq, less than 25 V, and less than 5 sec, respectively [1]. As presented in Table 1, the PC nanocomposite containing 0.5 wt% MWCNT without GNP loading had tribo-charge voltage outside the ESD specification. When 0.2-2.0 pph of resin of GNPs were added in the MWCNT/PC nanocomposite, the ESD properties were improved and were mostly within the range of the specification. However, the tribo-charge

Table 1. ESD results for compression-molded specimens based GNP/MWCNT/PC nanocomposites at different GNP contents.

GNP content (pph of resin)	Tribo-charge voltage (V)	Surface resistivity (Ω/sq)	Decay time (sec) from 1000 to 100 V	
			Positive charge	Negative charge
0	28.1±4.2	1.78±4.8 x 10^9	0.11 ± 0.08	0.20 ± 0.06
0.2	10.7±3.4	1.40±5.3 x 10^9	0.10 ± 0.04	0.16 ± 0.02
0.4	23.6±3.2	2.05±3.1 x 10^9	0.10 ± 0.05	0.10 ± 0.03
0.6	11.2±5.1	5.85±2.4 x 10^8	0.10 ± 0.01	0.10 ± 0.01
0.8	25.2±3.3	2.57±6.2 x 10^8	0.17 ± 0.03	0.14 ± 0.03
1.0	7.1±2.7	2.43±3.5 x 10^8	0.11 ± 0.02	0.12 ± 0.02
1.5	13.7±2.5	2.22±4.0 x 10^8	0.11 ± 0.04	0.10 ± 0.01
2.0	10.1±3.8	1.95±3.7 x 10^8	0.10 ± 0.02	0.13 ± 0.01

voltage did not show any clear trend with increasing GNP contents due to the variation of distribution and intercalation levels of GNPs in nanocomposites. Du et al. [38] presented that uniform distribution and low aggregation of carbon fillers in polymer matrix caused a segregated network structure, resulting in high conducting network formation at low filler loading. In addition, the increase of GNP content did not significantly affect the conductivity of the nanocomposite since the resistivity change may be still in the steepness range (the percolation threshold) of the percolation curve. The percolation threshold indicates the critical amount of filler necessary to initiate a continuous conductive network, which varies from polymer to polymer for a given conductive filler type [1].

3.5 Thermal Properties

Thermal stability is very important for polymeric materials as it is often the limiting factor both in processing and in end-use applications. Figure 4 shows the DSC heating thermogram of GNP/MWCNT/PC nanocomposites at various GNP concentrations. An apparent glass transition region was observed in curves of the samples. The T_g values of PC nanocomnposites were around 146-147°C as shown in Table 2. The T_g remained almost constant with the addition of MWCNTs and the mixture of MWCNTs and GNPs compared to PC resin (T_g = 146°C). The heat capacity jump at the glass transition stages was quite constant with increasing GNP content, which was approximately 0.21-0.23 J.(g polymer)$^{-1}$.C^{-1} (see Table 2). It was reported in the previous study that the heat capacity jump at the glass transition stages strongly decreased with increasing GNP content. It can be inferred that GNP restricted the motion of a significant fraction of polymer chain segments, preventing their participation in the glass transition process. However, those chains that can participate in the glass transition do not affect the T_g [39].

Thermal degradation of PC resin and PC nanocomposites with different weight fractions of GNPs was determined from weight loss measurement during heating. Figure 5 shows the TGA curves of GNP/MWCNT/PC nanocomposites. The T_d of GNP/MWCNT/PC nanocomposites changed marginally relative to that of pure PC (T_d = 530°C), as summarized in Table 2. Thermal degradation of the neat PC and its nanocomposites occurs as a single step process, with a maximum decomposition temperature at around 535°C. The addition of GNPs increased the thermal stability by around 5°C and 2-3°C compared with PC resin and MWCNT/PC nanocom-

Table 2. Thermal properties of GNP/MWCNT/PC nanocomposites at different GNP contents.

GNP content (pph of resin)	$T_{on\ set}$ (°C)	T_{mid} (°C)	T_{end} (°C)	Change in heat capacity J. (g polymer)$^{-1}$. C^{-1}	T_d (°C)
0	144.2	147.0	151.30	0.22	532.5
0.2	143.7	146.8	151.6	0.22	534.1
0.4	143.4	146.1	150.7	0.23	535.3
0.6	143.7	146.8	151.1	0.22	532.9
0.8	144.5	147.4	152.0	0.21	527.2
1.0	143.3	146.4	151.2	0.23	528.9
1.5	143.2	146.0	151.1	0.22	523.0
2.0	143.4	146.1	151.0	0.23	524.0

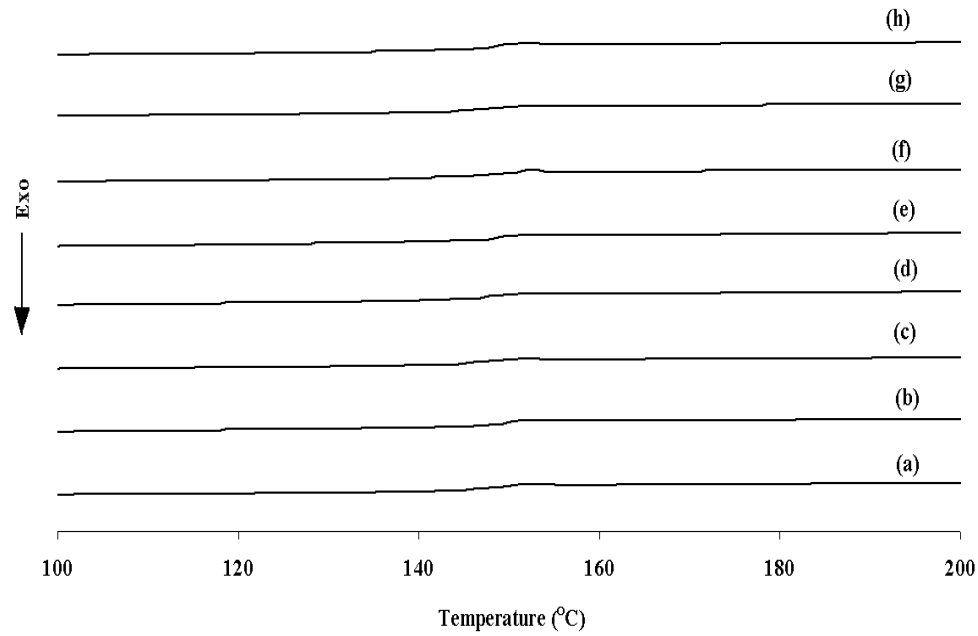

Figure 4. DSC curves of GNP/MWCNT/PC nanocomposites with the different GNP contents (pph of resin): (a) 0, (b) 0.2, (c) 0.4, (d) 0.6, (e) 0.8, (f) 1.0, (g) 1.5, and (h) 2.0.

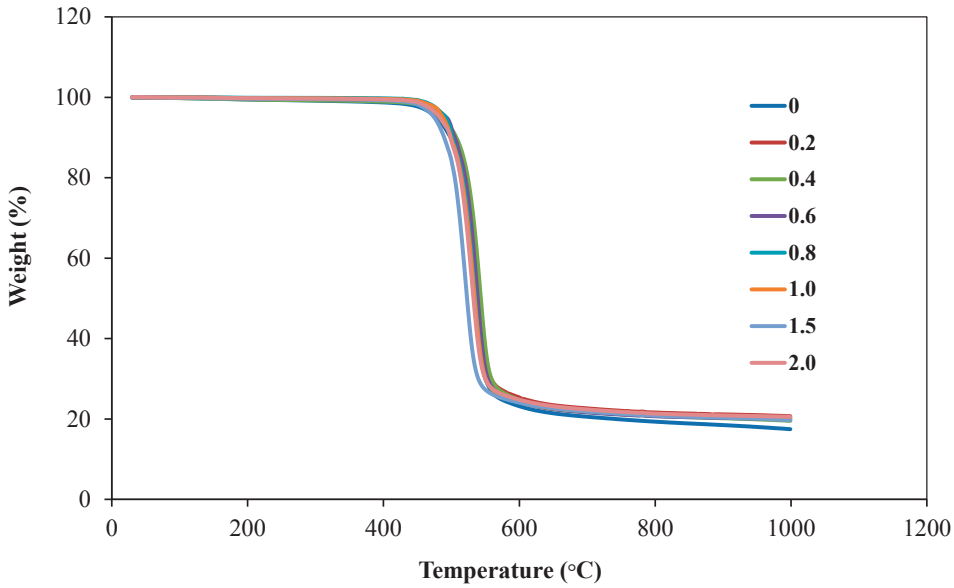

Figure 5. TGA curves of GNP/MWCNT/PC nanocomposites with the different GNP contents (pph of resin).

posite, respectively. However, the T_d began to decrease as the content of GNPs increased from 0.6 to 2.0 pph of resin. This might result from poor dispersion of GNPs in the PC matrix causing hot spot defects (aggregation and unintercalation of GNPs in a stacked morphology). The improvement in the resistance to thermal degradation at low content of GNP can be attributed to the hindered diffusion of volatile decomposition products within the nanocomposites, and it is strongly dependent on the MWCNT-polymer chains interactions [16]. The GNPs can be incorporated into a PC matrix by melt blending without any noticeable degradation, since they exhibit sufficient thermal stability in the range where polymer processing is performed.

3.6 MFI Measurement

The MFI of GNP/MWCNT/PC nanocomposites decreased from 37.6 to 19.5 g/10 min and 25.6 to 19.5 g/10 min as the content of GNPs increased from 0.2 to 2.0 pph of resin compared to neat PC resin and MWCNT/PC nanocomposite, respectively (see Figure 6). However, the MFI of the composites did not proportionally decrease with increasing of GNP content due to poor dispersion and intercalation of GNPs in the polymer matrix. The decrease in MFI suggested that the viscosity of the systems increased with addition of the GNPs. A transition from a liquid-like to a solid-like behavior occurred due to the formation of a nanoplatelet network which obstructed the motion of polymer chains [40]. Adding nanoplatelets, generally causes a large energetic barrier for segmental motions of polymer chains in the confined space and thus increases flow activation energy. In addition, Gu et al. [41] revealed that strong interactions between polymer matrix and fillers may also cause greater activation energies of flow. GNP fillers have a greater effect on flow because they have high aspect ratios and their alignment during flow is not possible [42].

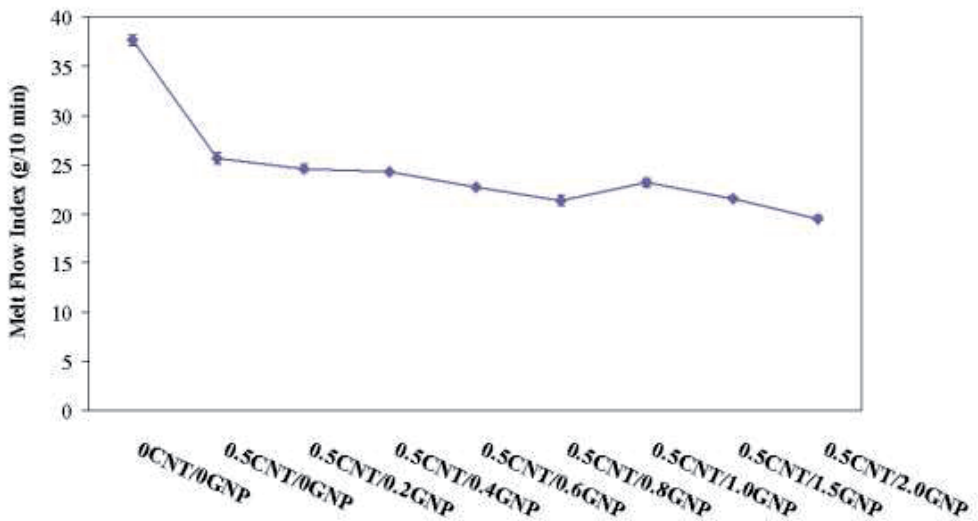

Figure 6. MFI results of PC resin and GNP/MWCNT/PC nanocomposites at different contents of GNP (pph of resin) at 260°C.

4. Conclusions

The mixtures of MWCNT (0.5 wt%) and various concentrations of GNP (0-2.0 pph of resin) were blended into PC resin by melt compounding using a twin-screw co-rotating extruder. Electrical and thermal properties as well as the MFI behavior of the obtained nanocomposites were compared to neat PC and/ or the MWCNT/PC composite to evaluate the impact of GNP additions. Electron microscopy and X-ray diffraction revealed slightly intercalated morphology and poor dispersion of GNPs in the base PC, resulting in variation of nanocomposite properties. The GNP/MWCNT/PC nanocomposites mostly exhibited the ESD properties in the specification range. The T_g and heat capacity jump at the glass transition stages of nanocomposites were insignificantly changed compared to that of the PC resin. The T_d value of nanocomposites increased at low content of GNPs but it decreased at high GNP loadings due to poor dispersion and intercalation of GNPs in the PC matrix causing hot spot defects. The addition of GNPs to the PC matrix resulted in decreasing MFI implying increasing melt viscosity.

The present study demonstrates that the GNP/MWCNT/PC nanocomposite with low loading of nanofillers is a promising material candidate for the next generation of ESD composite applications. Surface modification of GNPs such as oxygen plasma treatment, oxidation with acid, and reduction with base will be further studied to improve their dispersion and intercalation in the PC matrix.

Acknowledgements

The authors would like to acknowledge National Science and Technology Development Agency (NSTDA), Thailand for laboratory testing.

References

[1] Narkis M., Lidor G., Vaxman A. and Zuri L., New Injection moldable electrostatic dissipative (ESD) composites based on very low carbon black loadings, *J. Electristat.*, 1999; **47:** 201-214.

[2] Petrović Z.S., Martinović B., Divjaković V. and Budinski–Simendić J., Polypropylene–carbon black interaction in conductive composites, *J. Appl. Polym. Sci.*, 1993; **49:** 1659-1669.

[3] Collins P.G. and Avouris P., Nanotubes for electronics, *Sci. Am.*, 2000; **283:** 62-69.

[4] Nilsson J., Neto A.C., Guinea F. and Peres N., Electronic properties of graphene multilayers, *Phys. Rev. Lett.*, 2006; **97:** 266801.

[5] Balandin A.A., Ghosh S., Bao W., Calizo I., Teweldebrhan D., Miao F. and et al., Superior thermal conductivity of single-layer graphene, *Nano Lett.*, 2008; **8:** 902-907.

[6] Poot M. and Van der Zant H.S., Nanomechanical properties of few-layer graphene membranes, *Appl. Phys. Lett.*, 2008; **92:** 063111-063113.

[7] Dresselhaus M., Dresselhaus G., Charlier J. and Hernandez E., Electronic, thermal and mechanical properties of carbon nanotubes, *Philos. T. Roy. Soc. A.*, 2004; **362:** 2065-2098.

[8] Ruoff R.S. and Lorents D.C., Mechanical and thermal properties of carbon nanotubes, *Carbon*, 1995; **33:** 925-930.

[9] Jin S.H., Choi D.K. and Lee D.S., Electrical and rheological properties of polycarbonate/multiwalled carbon nanotube nanocomposites, *Colloid. Surface. A.*, 2008; **313:** 242-245.

[10] Spitalsky Z., Tasis D., Papagelis K. and Galiotis C., Carbon nanotube-polymer composites: Chemistry, processing, mechanical and electrical properties, *Prog. Polym. Sci.*, 2010; **35:** 357-401.

[11] Mahmoodi M., Arjmand M., Sundararaj U. and Park S., The electrical conductivity and electromagnetic interference shielding of injection molded multi-walled carbon nanotube/polystyrene composites, *Carbon*, 2012; **50:** 14554-14564.

[12] Li X., Wong S.Y., Tjiu W.C., Lyons B.P., Oh S.A. and He C.B., Non-covalent functionalization of multi walled carbon nanotubes and their application for conductive composites, *Carbon*, 2008; **46:** 829-831.

[13] Aussawasathien D. and Teerawattananon C., Preparation and properties of woven carbon fiber mat-epoxy composites containing dispersed base-functionalized multi-walled carbon nanotubes, *Chiang Mai J. Sci.*, 2012; **39:** 524-539.

[14] Aussawasathien D., Prakymoramas N. and Thanomjitr D., Effects of reprocessing on the structure and properties of polycarbonate/multi-walled carbon nanotube based electrostatic sissipative composites, *Chiang Mai J. Sci.*, 2013; **40:** 261-273.

[15] Xie S., Liu Y. and Li J., Comparison of the effective conductivity between composites reinforced by graphene nanosheets and carbon nanotubes, *Appl. Phys. Lett.*, 2008; **92:** 243121-243123.

[16] El Achaby M., Arrakhiz F.E., Vaudreuil S., El Kacem Q.A., Bousmina M. and Fassi-Fehri O., Mechanical, thermal, and rheological properties of graphene-based polypropyrene nanocomposites prepared by melt mixing, *Polym. Composite*, 2012; **33:** 733-744.

[17] Li W., Dichiara A. and Bai J., Carbon nanotube-graphene nanoplatelet hybrids as high-performance multifunctional reinforcements in epoxy composites, *Compos. Sci. Technol.*, 2013; **74:** 221-227.

[18] Liang J., Huang Y., Zhang L., Wang Y., Ma Y., Guo T. and et al. Molecular-level dispersion of graphene into poly(vinyl alcohol) and effective reinforcement of their nanocomposites, *Adv. Funct. Mater.*, 2009; **19:** 2297-2302.

[19] Balandin A.A., Ghosh S., Bao W., Calizo I., Teweldebrhan D., Miao F. and et al. Superior thermal conductivity of single-layer graphene, *Nano Lett.*, 2008; **8:** 902-907.

[20] Lier G.V., Alsenoy C.V., Doren V.V. and Greelings P., Ab initio study of the elastic properties of single-walled carbon nanotubes and graphene, *Chem. Phys. Lett.*, 2000; **326:** 181-185.

[21] Itkis M.E., Borondics F., Yu A. and Haddon R.C., Thermal conductivity measurements of semitransparent single-walled carbon nanotube films by a bolometric technique, *Nano Lett.*, 2007; **7:** 900-904.

[22] Zhu D., Bin Y. and Matsuo M., Electrical conducting behaviors in polymeric composites with carbonaceous fillers, *J. Polym. Sci. Pol. Phys.*, 2007; **45:** 1037-1044.

[23] Yi J.Y. and Choi G.M., Percolation behavior of conductor-insulator composites with varying aspect ratio of conductive fiber, *J. Electroceram.*, 1999; **3:** 361-369.

[24] Stankovich S., Dikin D.A., Dommett G.H., Kohlhaas K.M., Zimney E.J., Stach E.A. and et al., Graphene-based composite materials, *Nature*, 2006; **442:** 282-286.

[25] Ansari S. and Giannelis E.P., Functionalized graphene sheet-poly (vinylidene fluoride) conductive nanocomposites, *J. Polym. Sci. Pol. Phys.,* 2009; **47:** 888-897.

[26] Ramanathan T., Abdala A., Stankovich S., Dikin D., Herrera-Alonso M., Piner R. and et al., Functionalized graphene sheets for polymer nanocomposites, *Nat. Nanotechnol.*, 2008; **3:** 327-331.

[27] Eda G. and Chhowalla M., Graphene-based composite thin films electronics, *Nano Lett.*, 2009; **9:** 814-818.

[28] Kim H. and Macosko C.W., Processing-property relationships of polycarbonate/ graphene composites, *Polymer*, 2009; **50:** 3797-3809.

[29] Peigney A., Laurent C., Flahaut E., Bacsa R.R. and Rousset A., Specific surface area of carbon nanotubes and bundles of carbon nanotubes, *Carbon*, 2001; **39:** 507-514.

[30] Subrahmanyam K.S., Vivekchand S.R.C., Govindaraj A. and Rao C.N.R., A study of graphenes prepared by different methods: Characterization, properties and solubilization, *J. Mater. Chem.*, 2008; **18:** 1517-1523.

[31] Zeng Y., Ying Z., Du J.H. and H.M., Effects of carbon nanotubes on processing stability polyoxymethylene in Melt-mixing process, *J. Phys. Chem. C*, 2007; **111:** 13945-13950.

[32] Yao X., Wu H.X., Wang J., Qu S., Chen G., Carbon nanotube/poly(methyl methacrylate) (CNT/PMMA) composite electrode fabricated by *in situ* polymerization for microchip capillary electrophoresis, *Chem. Eur. J.*, 2007; **13:** 846-853.

[33] Lee Y.R., Raghu A.V., Jeong H.M. and Kim B.K., Properties of water-borne polyurethane/functionalized graphene sheet nanocomposites prepared by an *in situ* method, *Macromol. Chem. Phys.*, 2009; **210:** 1247-1254.

[34] Tuinstra F. and Koenig J.L., Raman spectrum of graphite, *J. Chem. Phys.*, 1970; **53:** 1126-1130.

[35] Chieu, T. and Dresselhaus, M.S., Raman studies of benzene-derived graphite fibers, *Phys. Rev. B*, 1982; **26:** 5867-5877.

[36] Gao, C., Jin Y.Z., Kong, H., Whitby, R.L.D., Acquah, S.F.A., Chen G.Y., Qian, H.H., Hartschuh, A., Silva, S.R.P. and et al., Polyurea-functionalized multiwalled carbon nanotubes: Synthesis, morphology, and Raman spectroscopy, *J. Phys. Chem. B*, 2005; **109:** 11925-11932.

[37] Zhang H-B., Zheng W-G., Yan Q., Yang Y., Wang J-W., Lu Z-H., Ji G-Y. and Yu Z-Z., Electrically conductive polyethylene terephthalate/ graphene nanocomposites prepared by Melt compounding, *Polymer*, 2010; **51:** 1191-1196.

[38] Du J., Zhao L., Zeng Y., Zhang L., Li F., Liu P. and Liu C., Comparison of electrical properties between multi-walled carbon nanotube and graphene nanosheet/high density composites with a segregated structure, *Carbon*, 2011; **49:** 1094-1100.

[39] Zhan Y., Wu J., Xia H., Yan N., Fei G. and Yuan G., Dispersion and exfoliation of graphene in rubber by an ultrasonically-assisted latex mixing and *in situ* reduction process, *Macromol. Mater. Eng.*, 2011; **296:** 590-602.

[40] Aalaie J., Rahmatpour A. and Maghami S., Preparation and characterization of linear low density polyethylene/carbon nanotube nanocomposites, *J. Macromol. Sci. B*, 2007; **46:** 877-889.

[41] Gu S.Y., Ren J. and Wang Q.F., Rheology of poly(propylene)/ clay nanocomposites, *J. Appl. Polym. Sci.*, 2004; **91:** 2427-2434.

[42] Barus S., Zanetti M., Bracco P., Musso S., Chiodoni A. and Tagliaferro A., Influence of MWCNT morphology on dispersion and thermal properties of polyethylene nanocomposites, *Polym. Degrad. Stab.*, 2010; **95:** 756-762.